PROCEEDINGS, Twenty-Eighth Workshop on Geothermal Reservoir Engineering
Stanford University, Stanford, California, January 27-29, 2003
SGP-TR-173

INVERSE MODELING OF FRACTURED GEOTHERMAL RESERVOIRS USING PRESSURE INTERFERENCE DATA

Shinsuke Nakao, John W. Pritchett*, and Tsuneo Ishido

Geological Survey of Japan, AIST
1-1-1 Higashi
Tsukuba, Ibaraki, 305-8567, Japan
e-mail: sh-nakao@aist.go.jp

* Science Applications Int'l. Corp.
10260 Campus Point Dr.
San Diego, CA 92121

ABSTRACT

Numerically inverting simultaneous pressure-interference measurements from multiple observation wells can help to establish the large-scale spatial distributions of permeability and storage within a geothermal reservoir. For realistic results, it is important to incorporate double-porosity (MINC) descriptions into the modeling process to properly reproduce the short-term pressure-transient response to production or injection. A new finite-difference inversion program has been developed for this purpose. The reservoir is represented as a three-dimensional network of grid blocks, and the description is restricted to single-phase (liquid) flow. The single-phase limitation permits the linearization of the pressure-diffusion equation in the sub-grid "matrix region", so that MINC descriptions may be accommodated at little additional computing cost. The "simulated annealing" method is used as the optimizing technique.

INTRODUCTION

Numerical models of geothermal reservoirs can be useful for both resource evaluation and forecasting future performance. Such models are usually constructed iteratively, varying the pertinent formation properties in each grid block from case to case so that an accurate representation gradually evolves. This process is necessarily time-consuming.

Pressure interference testing using multiple production/injection/observation wells may in principle be used to evaluate transmissivity and storativity of a geothermal reservoir. Once pressure transient data are obtained, the records may be inverted numerically to help establish the large-scale spatial distributions of permeability and storage within the system. These results, intermediate between traditional semi-analytic ("type-curve") pressure-transient interpretation techniques and detailed nonlinear distributed-parameter reservoir models, can then be used as a starting point for detailed numerical reservoir modeling studies. In this way, the trial-and-error effort required for large-scale model development may be reduced.

The *"simulated annealing"* (SA) method is used as the optimizing technique. SA is a stochastic search method that has been effective for a variety of optimization problems (Kirkpatrick *et al.,* 1983), including groundwater management hydrology studies (Dougherty and Marryott, 1991), stochastic reservoir modeling (Deutsch and Journel, 1994), and fracture network modeling in igneous rocks (Mauldon *et al.,* 1993; Najita and Karasaki, 1995; Nakao *et al.,* 1999).

For realistic results, it is important to incorporate double-porosity (MINC) descriptions (Pruess and Narasimhan, 1985) into the modeling process to properly reproduce the short-term pressure-transient response to production or injection arising from the (usually) fracture-dominated character of geothermal reservoirs. In this paper, we start with a brief general description of SA, and then proceed to describe how we use SA for well-test inversion. Finally, numerical examples are presented.

SIMULATED ANNEALING

SA has its origins in thermodynamics and the manner in which liquid metals cool and anneal. In physical annealing, a metal is heated and then allowed to cool very slowly in order to obtain a regular molecular configuration having the lowest possible energy state. If the temperature (T) is held constant, the system approaches thermal equilibrium and the probability distribution for the configuration with energy E

approaches the Boltzmann distribution. Metropolis *et al*. (1953) first introduced an algorithm to incorporate these ideas into numerical calculations. The following criterion (known as the Metropolis algorithm) is applied to determine whether a transition to another configuration will occur at the current temperature. For the $(n-1)^{th}$ configuration X_{n-1} and the n^{th} configuration X_n (with energies E_{n-1} and E_n respectively), the transition probability at a particular system temperature T is given by

$$\begin{aligned} &\Pr(X_{n-1} \rightarrow X_n) \\ &= 1 \qquad\qquad \text{if } E_n - E_{n-1} \le 0 \\ &= \exp[-(E_n - E_{n-1})/k_b T] \quad \text{if } E_n - E_{n-1} > 0 \end{aligned} \qquad (1)$$

This criterion *always* allows a transition to the new configuration if system energy decreases, and *sometimes* permits a transition even if energy increases. This stochastic relaxation step allows SA to search the space of possible configurations without always just converging to the nearest local minimum. In SA, the objective ("error") function for an optimization problem is analogous to *"energy"* and the set of free parameters *("configuration")* is analogous to the arrangement of molecules. "*Temperature*" is simply a control parameter in a given optimization problem.

In general, the SA algorithm consists of the following sequence of steps: (1) generate or randomly change the system configuration, (2) calculate values of the objective function (energy) for both the "old" and "proposed new" states, (3) use the Metropolis algorithm to determine whether the new configuration is accepted or not, and (4) adjust the current control parameter T according to the preset annealing (cooling) schedule.

Several choices of annealing schedule are possible. A computationally practical schedule is the widely used "decrement rule". Given an initial control parameter value T_0, assign

$$T_k = T_0 \alpha^k; \; k = 0,1,2,3 \ldots, \qquad (2)$$

where α is between 0 and 1. This general form has been used in various applications with values of α ranging from 0.5 to 0.99 (e.g., van Laarhoven and Aarts, 1987). In this schedule, the current control parameter T is kept fixed until a finite number of transitions, L_k, have been accepted, then the T parameter is reduced.

APPLICATION TO PRESSURE-TRANSIENTS

In order to use SA for the inversion of well tests, the reservoir is represented as a three-dimensional network of finite-difference grid blocks, and the description is restricted to single-phase (liquid) flow. The single-phase limitation permits the linearization of the pressure-diffusion equation in the sub-grid "matrix region", so that MINC descriptions may be accommodated at little additional computing cost (Pritchett, 1997). Although SA is generally more effective that other methods at finding a globally optimum inverse result and avoiding local minima, more iterations (and computer time) are usually required, so that rapid solution algorithms are a priority. Both flowing wells and observation wells communicate with the reservoir at their feedpoints, which are treated as infinitesimal points lying within the grid volume. For each iteration, complete pressure transient histories due to production or injection are calculated for each grid block using the finite difference code (Pritchett, 1997).

To invert the data, the objective is to find a near-optimal reservoir model by modifying rock properties of clusters of grid blocks and calculating pressure transient curves in order to simultaneously match observed data at observation wells. The approach of changing a cluster of grid blocks follows the work of Jacobsen (1993), and Najita and Karasaki (1995). At each step of the algorithm, a cluster of grid blocks is randomly selected and new properties are randomly chosen from a pre-defined "candidate list" (of finite length) and assigned to all grid blocks in the cluster. The number of entries on the "candidate list" and the values of rock properties in each entry are user-specified.

Available types of candidate rock descriptions include a "*porous-medium*" model, a "*conventional MINC*" double-porosity model and a "*heterogeneous MINC*" model (which involves a spectrum of fracture separation values within a single computational grid block). Provision is also made for "*impermeable"* and "*fixed-pressure*" grid blocks to be incorporated in the candidate list. The formation storage value ("$\phi\rho C$") and the transmissivities in the x-, y- and z-directions ("$k_i\rho/\mu$") must be provided, where ρ, μ, C and k_i are fluid mass density, fluid dynamic viscosity, reservoir compressibility and formation permeability in the i-direction (i = x, y, z), respectively. For the MINC models, matrix region storage fraction(s) and "characteristic drainage time(s)"

$$\tau_c = \phi_m C_m \mu \lambda^2 / 4k_m \qquad (3)$$

(subscript "m" signifies "matrix region") must also be specified.

It should be noted that the computer program applies "fixed-pressure" (Dirichlet-type) boundary conditions to all six exterior surfaces of the computational grid. Therefore, if "impermeable" (Neumann-type) exterior boundaries are desired instead along part or all of the exterior surfaces, "impermeable" grid blocks may be placed along the boundaries to impose those conditions. The user may specify particular grid blocks as "fixed" (not subject to variation in rock properties during the inversion) to maintain boundary

conditions and/or to reflect independent information about the reservoir.

Following the perturbation step, well tests are simulated and the calculated pressure transients are compared with observed data. The objective function (energy) to be minimized is a dimensionless squared weighted difference between the calculated and observed downhole pressures. The Metropolis algorithm is applied to determine whether the current reservoir configuration is acceptable based on Eq. (1). When L_k acceptable transitions (at T_k) have been achieved, the "temperature" is reduced to T_{k+1} using equation (2). T_{k+1} stays constant until L_{k+1} transitions have been accepted at T_{k+1}. This process continues until the annealing schedule is exhausted or the number of iterations has reached a user-specified maximum. At this point, the best model found thus far is hopefully close to the global minimum.

NUMERICAL EXAMPLES

To illustrate, we present inversion results using synthetic reservoir models to investigate the method's behavior and to evaluate its potential as an inversion technique. Although the reservoir model (transmissivity/storage distribution) is rather simple for these synthetic cases, the actual reservoir structure is known exactly, so that the effectiveness of the inversion procedure can be appraised.

Case 1

First, consider a horizontal region (1000 m × 1000 m in area and 300 meters thick) filled with 100 m × 100 m × 100 m cubical grid blocks (300 blocks total). The upper and lower layers are designated impermeable, so that properties are varied only within the middle layer (100 blocks) and the problem is two-dimensional. The "real" reservoir consists of two formations with the same transmissivity ("kρ/μ" = 6.45×10^{-8} s; k = 10^{-14} m^2); but one is porous and the other is a MINC-type fractured medium (τ_c = 20 hour), as shown in Figure 1. Pulse testing with 12, 24, and 48-hour injections at 600 kg/min was simulated at the central well and pressure transients were observed at the injection well and the surrounding four shut-in observation wells (case 1B). To examine the effect of flow-rate history, a 3.5-day constant rate case was also considered (case 1A). Five types of candidate rock formation are involved: "impermeable" rock, "fixed-pressure" rock, and three candidates with transmissivity ("kρ/μ") = 6.45×10^{-8} seconds; a "porous medium", a "MINC medium" with τ_c = 20 hours and another "MINC" formation with τ_c = 100 hours. Storativity ("ϕρC") is 10^{-7} s^2/m^2 for all formations. Initially, the entire system is impermeable. The "cluster size" is constrained to lie between 1 and 10 blocks.

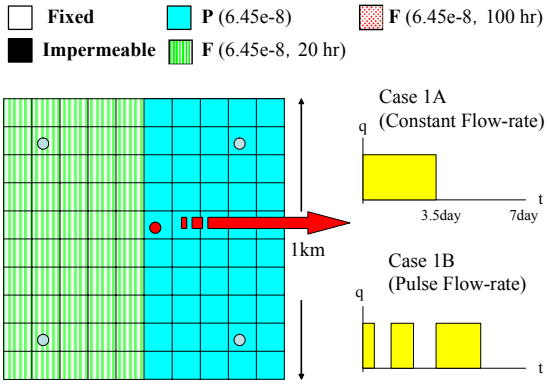

Figure 1. Synthetic "real" reservoir for case 1, injection flow-rate histories and candidate rock formations.

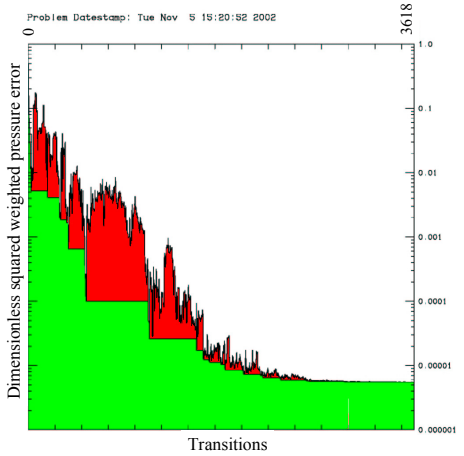

Figure 2. Objective function versus transitions for case 1B.

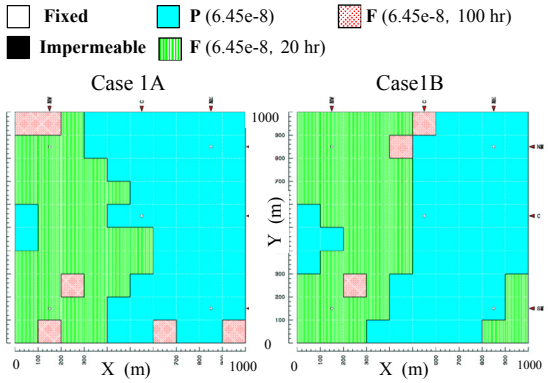

Figure 3. Inversion results for case 1A (left) and case 1B (right).

The inversion was run for 20000 iterations. The control parameter T was adjusted according to Eq. (2) using $\alpha = 0.9$, starting from $T_0 = 0.1$. Objective functions below 10^{-5} were achieved at 15872 and 19139 iterations for cases 1A and 1B, respectively. A plot of objective function (energy) versus transition number for the inversion of case 1B is shown in Figure 2. Note that the Metropolis algorithm permits many transitions involving objective function increases within an overall decreasing trend. Figure 3 shows the "best" solutions found in these two cases at this stage. Both do a reasonably good job of replicating the "exact" result (Figure 1).

Case 2

The second case uses the same grid geometry and boundary conditions, but the "real" transmissivity distribution is somewhat more complex and, in addition, random perturbations (amplitude 5% of maximum signal for each trace) were added to the synthetic "pressure observations" to simulate measurement errors. Six rock formations were specified for the "candidate list", consisting of (a) porous media and (b) MINC media (τ_c = 20 hours), with three different values of transmissivity "kρ/μ": (a) the same as used in Case 1 (6.45×10^{-8} seconds), (b) a value ten times greater, and (c) a value one-tenth that of Case 1. The "real" reservoir was considered to consist of four of these formations (both "porous" and "MINC" medium-transmissivity formations, and the "MINC" version of both the low- and high-transmissivity formations), arranged in a checkerboard pattern as indicated in Figure 4. Fluid was injected at 600 kg/min into the central well for 3.5 days, followed by 3.5 days of falloff. Pressure traces are available for all five wells. As before, the system is initially impermeable, the "cluster size" is constrained to lie between 1 and 10 blocks, and the "maximum iterations" value and the annealing schedule are the same as for Case 1.

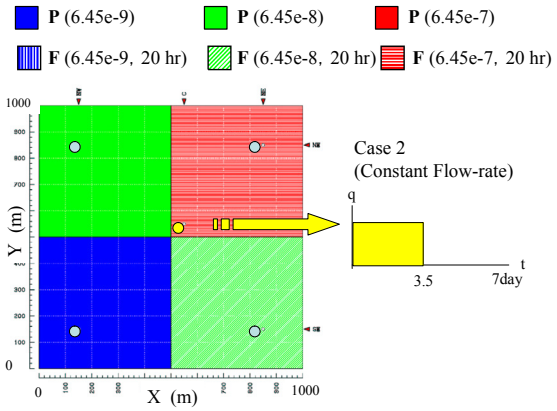

Figure 4. Synthetic "real" reservoir for case 2, injection flow-rate history and candidate rock formations.

The objective function dropped to ~10^{-4} after 17694 iterations (with no further improvement to 20000 steps). Comparison of the pressure interference signal between synthetic (and randomly perturbed) "observed" data and computed results are shown for one of the observation wells in Figure 5; the fit is fairly good, considering the data scatter. Figure 6 illustrates the final computed distribution of formation properties. Although the area occupied by the medium-transmissivity formations is underestimated somewhat, the general locations of the various structures are reasonably well reproduced. Naturally, the greater the amount of "measurement error", the greater the deviations between "real" and "inverted" geological structures are likely to be.

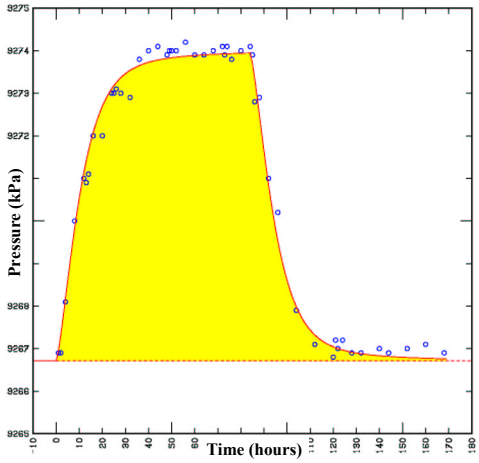

Figure 5. Comparison of pressure interference response between synthetic "observed" data and inversion result for one of the observation wells (case 2).

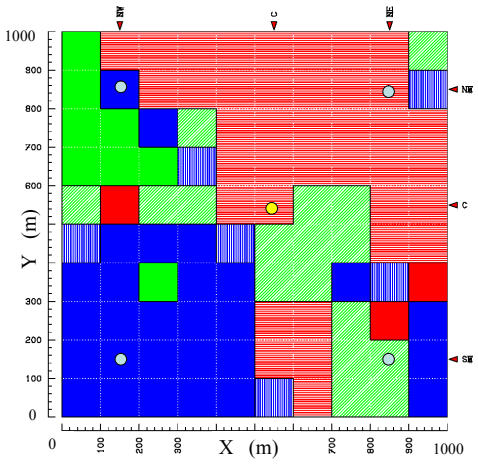

Figure 6. Inversion result for case 2.

REFERENCES

Deutsch, C.V. and Journel, A. G. (1994), "Integrating well test-derived effective absolute permeability in geostatistical reservoir modeling," *Stochastic modeling and geostatistics*, Yarus, J. M. and R. L. Chambers (Eds.), AAPG, 131-141.

Dougherty, D. and Marryott, R. A. (1991), "Optimal groundwater management, 1, Simulated annealing," *Water Resources Research*, **27**, 2493-2508.

Jacobsen, J. S. (1993), *"A user's and programmer's guide to anneal: a research code developed to implement simulated annealing for hydraulic well test applications,"* Technical report, Lawrence Berkeley Laboratory, Berkeley, 58pp.

Kirkpatrick, S., C. D. Gelatt, Jr., and Vecchi, M. P. (1983), "Optimization by simulated annealing," *Science*, **220**, 671-680.

Mauldon, A. D., K. Karasaki, S. J. Martel, J. C. S. Long, M. Landsfeld, A. Mensch, and S. Vomvoris. (1993), "An inversion technique for developing models for fluid flow in fracture systems using simulated annealing," *Water Resources Research*, **29**, 3775-3789.

Metropolis, N., A. Rosenbluth, M. Rosenbluth, A. Teller and E. Teller. (1953), "Equation of state calculations by fast computing machines," *Journal of Chemical Physics*, **21**, 1087-1092.

Najita, J. and K. Karasaki. (1995), *"Inversion of hydraulic well tests using cluster variable aperture simulated annealing,"* Lawrence Berkeley National Laboratory report LBNL-39111, Berkeley, 43pp.

Nakao, S., J. Najita, and K. Karasaki. (1999), "Sensitivity study on hydraulic well testing inversion using simulated annealing," *Ground Water*, **37**, 736-747.

Pritchett, J. W. (1997), "Efficient numerical simulation of nonequilibrium mass and heat transfer in fractured geothermal reservoirs," *Proc. 22nd Workshop on Geothermal Reservoir Engineering,* Stanford Univ., 287-293.

Pruess, K. and Narasimhan, T. N. (1985), "A practical method for modeling fluid and heat flow in fractured porous media," *Soc. Pet. Eng. J.*, February, 14-26.

van Laarhoven, P. J. M. and E. H. L. Aarts. (1987), *Simulated Annealing: Theory and Applications*. D.Reidel Publishing Co., 186pp.